Energy Transfer in Dual MHD Convection of Heat and Mass Flow of Cu – H_2O Nanofluid in a Porous Channel with Oscillating Upper Plate

Amadi, Okechukwu(PhD)
Department of Mathematics/Statistics, Ignatius Ajuru University of Education, P.M.B 5047 Rumuolumeni, Nigeria
agirobert@gmail.com

DOI: 10.56201/ijcsmt.v8.no2.2022.pg32.49

Abstract

The study investigated thermal transfer in MHD convective flow of Cu-H_2O nanofluid in a porous medium with heat generation/absorption. A set of partial differential equations with copper nanoparticles were used. The partial differential equations were non-dimensioned with various dimensionless quantities in order to obtain forms whose solutions can be easily obtained. The partial differential equations were later transformed into ordination differential equations through a two term perturbation technique which were later solved using method of undetermined coefficient to obtain the exact solutions for the energy, concentration and momentum equations. Using the exact solutions; plots were done with the aid of standard parameters to estimate the variational effects of parameters that entered the flow field and from the plots; it was observed that thermal radiation decreased the temperature of the fluid. Heat generation/absorption parameter increased the temperature of the fluid. The effective thermal conductivity increased the temperature of the fluid. Peclet number decreased the velocity of the fluid. Reynolds number decreased the fluid velocity, increasing the Schmidt number, frequency of oscillation increase the concentration of the fluid.

***Keywords**: Heat and Specie transfer, Heat generation, Nanofluid, Magnetohydrodynamics(MHD)*

I. INTRODUCTION

Warm conductivity assumes a fundamental part in warmness move upgrade. Regular intensity switch liquids alongside water, ethylene glycol (EG), lamp oil and ointment oils have negative warm conductivities contrasted with solids. Solids trash anyway has better warm conductivities in contrast with conventional warmth switch liquids. Choi (1995) in his spearheading works of art demonstrated that when a little amount of nanoparticles .is added to be expected base liquids, it will increment broadly the warm conductivity of the base liquids notwithstanding their convective warmness move rate. This blend is known as nanofluids. All the more definitively, nanofluids are suspensions of nano-length garbage in base liquids. Typically nanofluids incorporate explicit kinds of nanoparticles comprehensive of oxides, metals and carbides in for the most part base liquids like water, EG, propylene glycol and lamp oil. A few extraordinary bundles of nanofluids are situated in different computerized hardware, energy supply, energy age, air con and assembling. Vajjha and Das (2009) interestingly utilized EG (60 %) and water (forty %) total as base liquid for the readiness of alumina (Al2O3), copper oxide (CuO) and zinc oxide (ZnO) nanofluids. At the indistinguishable temperature and consideration, they saw that CuOnanofluidgangs unreasonable warm conductivity assess to the ones of Al2O3 and ZnOnanofluids. Naik and Sundar (2011) took 70 % propylene glycol and 30 % water and arranged CuOnanofluid. True to form, they found that CuOnanofluid has better warm conductivity and thickness homes contrast with base liquid. Malvandi et al.(2013) concentrated on entropy age of nanofluids over a plate scientifically. The utilized the homotopy-pertubation strategy (HPM) and the variational emphasis technique (VIM) to settle the nonlinear customary differential condition. It was noticed the high thickness of Cu adding this nanoparticles to water produces more entropy rather than other nanoparticles in a cycle. Thiagarajan et al.(2019) set out on the review thick dissemination and joule warming consequences for thermo solutal defined nanofluid over an extending sheet. They commented that Schmidt number reductions the temperature subsequent to getting a mathematical arrangement of the nonlinear conventional differential conditions. Md et al.(2012) concentrated on the insecure mhd free convection of nanofluid along an extending sheet with warm radiation. They acquired different time steps and for the various upsides of the boundaries of physical and designing interest. Normal convection stream of partial nanofluids over an isothermal vertical plate with warm radiation was concentrated by Constantin et al.(2017). The liquid temperature increments for expanding upsides of the nanoparticle volume division was noted by them subsequent to acquiring the shut structure arrangement and plotting the diagram. Latiff et al.(2016) concentrated on Stefan blowing impact of nanofluid over a strong pivoting stretchable circle. The nonlinear normal differential conditions were addressed mathematically utilizing the Runge-Kutta-Fehlberg technique. It was commented that the Stefan blowing builds the nearby skin contact and diminishes the intensity move, mass exchange and microorganism move rates. Second request slip stream of Cu-Water nanofluid over an extending sheet with heat move was gone through by Rajesh et al.(2014). They settled the differential conditions utilizing limited component technique. They show the impacts of boundaries variety with the guide of diagrams. Aaiza et al.(2015) concentrated on energy move in nanofluid containing various states of nanoparticles. They found that thickness and warm conductivity ate the most unmistakable boundaries answerable for various consequences of speed and temperature.

The idea of intensity producing and engrossing liquid can't be overlooked because of its importance in issues managing compound responses. Heat age impacts might change the temperature dissemination asnd this thus can affect the molecule testimony rate in atomic reactors, electronic chips and semi guide wafers. However the specific displaying of inward intensity age or retention in its sense is challenging to battle yet a few straightforward numerical models can be utilized to communicate its overall way of behaving for a large portion of the actual conditions. It is thought to be steady, space-ward or temperature - subordinate. A large group of creators have managed this idea. Thiagarian et al.(2019) concentrated on gooey scattering of nanofluid over an extending sheet with heat age. They settled the nonlinear models taking on a mathematical methodology of Nachitsheim-Swigert shooting strategy conspire along with RungeKutta fourth request. Strikingly they noticed that heat age expanded the temperature of the liquid viable. Mass exchange and intensity age impacts was set out on by Reddy et al.(2011). They considered the mhd free convection in association with it. They embraced the RungeKutta fourth request with shooting method to take care of the issues. They noticed that heat age expanded both the speed and temperature of the liquid.

Magnetohydrodynamics (MHD) is the science which is related with the movement of really leading fluids within the sight of an attractive field. The movement of the directing fluid all through the attractive region creates electric flows which change the attractive field, and the movement of the attractive field on those flows offers up push to mechanical powers which adjust the float of the fluid. MHD joins the two norms of liquid elements and electromagnetism. MHD considers the attractive properties of electrically directing liquids. When an electrically leading liquid travels through an attractive field, an electric field might be welcomed on and will connect with the attractive properties to supply a body pressure. The science which manages this peculiarity is alluded to as magnetohydrodynamics. Attributable to the meaning of this idea; such countless creators divide dove into it. Soret impact on MHD free convection through a permeable slanted channel was set out upon by Achogo et al.(2020). They noticed that soret number increments both the focus and speed profiles in the wake of getting the shut structure systematically through the technique for dubious coefficient. Reddy et al.(2011) inspected mass exchange and intensity age impacts on MHD free convection stream past a slanted vertical surface ina permeable medium. They settled the nonlinear frameworks through a mathematical methodology by applying the Runge-Kutta strategy for fourth request with shooting procedure. Buggaramulu et al.(2017) concentrated on MHD convection stream of Kuvshinski liquid beyond an endless vertical porus plate. The nonlinear conditions were tackled by embracing a two term irritation procedure and they settled scientifically.

In this paper, we considered the energy transfer in dual mhd convection of heat and mass flow of cu – h_2o nanofluid in a porous channel with oscillating upper plate.

II. FORMULATION OF THE PROBLEM

The following assumptions were made;

a) The flow is oscillatory of nanofluids.
b) The fluid is electrically conducting in the presence of uniform magnetic field applied perpendicularly to the direction of flow.
c) The magnetic Reynolds number is very small such that the impact of induced magnetic field is forfeited.
d) The external electric field is considered zero and the electric field due to polarization is negligible.
e) The no-slip condition at the boundary walls is considered.
f) The x-axis is taken along the flow and y-axis is taken normal to the direction of flow.
g) The natural convection results from buoyancy force together with external pressure gradient applied along the x-direction.
h) T_0 and T_w are considered very high enough to induce the radiative heat transfer.
i) C_0 and C_w are considered very high enough to induce mass transfer.
j) Going by the Boussinesq approximation, the governing equations of momentum and energy are as follows;

$$\rho_{nf}\left(\frac{\partial u'}{\partial t'}+v'\frac{\partial u'}{\partial y'}\right)=-\frac{\partial p'}{\partial x'}+\mu_{nf}\frac{\partial^2 u'}{\partial y'^2}-\frac{\mu_{nf}}{K}u'-\sigma\beta_0^2u'+g(\rho\beta)_{nf}(T'-T_0)+g(\rho\beta)_{nf}(C'-C_0) \quad (1)$$

$$\left(\rho c_p\right)_{nf}\left(\frac{\partial T'}{\partial t'}+v'\frac{\partial T'}{\partial y'}\right)= k_{nf}\frac{\partial^2 T'}{\partial y'^2}-\frac{\partial q_r'}{\partial y'}-Q_0(T'-T_0)$$
(2)

$$\left(\rho c_p\right)_{nf}\left(\frac{\partial C'}{\partial t'}+v'\frac{\partial C'}{\partial y'}\right)= D_{nf}\frac{\partial^2 C'}{\partial y'^2}-Kr'(C'-C_0)$$
(3)

Where u=u(y,t) represents the velocity in the direction of x, T=T(y,t) the temperature, C=C(y,t) the concentration, ρ_{nf} the density, μ_{nf} the dynamic viscosity of the nanofluid, σ the electrical conductivity of the base fluid, $K > 0$ the permeability of the porous medium, $(\rho\beta)_{nf}$ thermal expansion coefficient of nanofluid, g the acceleration due to gravity, $\left(\rho c_p\right)_{nf}$ the heat capacitance of nanofluids, k_{nf} the thermal conductivity of nanofluid, q_r the radiative heat flux in x-direction, p the external pressure, Q_0 the heat generation/absorption, Kr the chemical reaction term

The boundary condition expedient are as follows;

$y'=0;\ u'=0,\ T'=T_0,\ C'=C_0$ (4a)

$y'=d;\ u'=H(t)\varepsilon e^{i\omega' t'}\ ;\ t>0,\ T'=T_w,\ C'=C_w$ (4b)

Following the Hamilton and Crosser model(1962),the dynamic viscosity of the nanofluid(μ_{nf}), thermal expansion coefficient of nanofluid($(\rho\beta)_{nf}$), heat capacitance of nanofluids($\left(\rho c_p\right)_{nf}$), thermal conductivity of nanofluid(k_{nf}) are;

$$\mu_{nf}=\mu_f(1+a\emptyset+b\emptyset^2)$$
(4a)

$$\frac{k_{nf}}{k_f}=\frac{k_s+(n-1)k_f+(n-1)\left(k_s-k_f\right)\emptyset}{k_s+(n-1)k_f+\left(k_s-k_f\right)\emptyset}$$
(4b)

$$\rho_{nf}=(1-\emptyset)\rho_f+\emptyset\rho_s$$
(4c)

$$(\rho\beta)_{nf}=(1-\emptyset)(\rho\beta)_f+\emptyset(\rho\beta)_s$$
(4d)

$$\left(\rho c_p\right)_{nf}=(1-\emptyset)\left(\rho c_p\right)_f+\emptyset\left(\rho c_p\right)_s$$
(4e)

$\emptyset$ denotes the nanoparticles volume fraction, ρ_f and ρ_s are the densities of the base fluid and solid nanoparticles, β_s and β_f are the volumetric expansion coefficients of thermal expansions of solid nanopartiles and base fluids, $\left(c_p\right)_s$ and $\left(c_p\right)_f$ are the specific heat capacities of solid nanoparticles and base fluids at constant pressure, a and b represent constants and find their values on the particle shape as represented by Aaiza et al.(2015) in Table 1. The n in equation (4b) denotes the empirical shape factor and it is expressed as $n=\frac{3}{\Psi}$, where Ψ means the sphericity which denotes the ratio between the surface are of the sphere and the surface area of the real particle with equal volumes(Aiza et al.(2015)). The Ψ is clearly seen in Table 2.

Table1: Constants a and b empirical shape factors

Model	Platelet	Blade	Cylinder	Brick
A	37.1	14.6	13.5	1.9
B	612.6	123.3	904.4	471.4

Table 2: SphericityΨ for different shapes nanoparticles

Model	Platelet	Blade	Cylinder	Brick
Ψ	0.52	0.36	0.62	0.81

Table 3: Thermophysical properties of water and nanoparticles

Model	$\rho(kgm^{-3})$	$c_p(kg^{-1}K^{-1})$	$k(Wm^{-1}K^{-1})$	$\beta \times 10^{-5}(K^{-1})$
Pure water(H_2O)	997.1	4179	0.613	21
Copper(Cu)	8933	385.0	401.0	1.67

Following Cogley et al.(1968) for optically thin fluid with relatively low density, the heat flux is expressed as;

$$\frac{\partial q_r}{\partial y} = -4\alpha^2(T' - T_0) \quad (5)$$

The symbol α denotes the mean radiation absorption coefficient.

Now introducing equation (5) into equation (2), it yields;

$$\left(\rho c_p\right)_{nf}\left(\frac{\partial T\prime}{\partial t\prime} + v'\frac{\partial T\prime}{\partial y\prime}\right) = k_{nf}\frac{\partial^2 T\prime}{\partial y'^{\,2}} + 4\alpha^2(T' - T_0) - Q_0(T' - T_0) \quad (6)$$

Now we introduce the following dimensionless quantities into equations (1) and (6)

$$x = \frac{x'}{d}, y = \frac{y'}{d}, u = \frac{u'}{U_0}, t = \frac{tU_0}{d}, p = \frac{d}{\mu U_0}p', T = \frac{T' - T_0}{T_w - T_0}, C = \frac{C' - C_0}{C_w - C_0},, \omega = \frac{d\omega'}{U_0}, \varepsilon = \frac{\mu}{\mu_f},$$

$$\frac{\partial p}{\partial x} = \lambda e^{i\omega t}, Re = \frac{U_0 d}{v_f}, M^2 = \frac{\sigma B_0^2 d^2}{\mu_f}, K = \frac{K'}{d^2}, Gr = \frac{g\beta_f d^2(T_w - T_0)}{v_f U_0}, Pe_t = \frac{U_0 d\left(\rho c_p\right)_f}{k_f}, N^2 = \frac{4d^2\alpha^2}{k_f},$$

$$\lambda n = \frac{k_{nf}}{k_f}, S = \frac{Q_0 d^2}{k_f}, \eta = \frac{1}{U_0}, v = \frac{v\prime}{v_0}, Pe_c = \frac{U_0 d\left(\rho c_p\right)_f}{D_{nf}}, Gr = \frac{g\beta_f d^2(C_w - C_0)}{v_f U_0}, Sc = \frac{v}{D_{nf}}, Kr = \frac{Kr' d}{v}$$

together with equations (4a)-(4e) appropriately.

Re is the Reynolds number, M is the magnetic parameter also known as the Hartmann number, K is the permeability, Gr is the thermal Grashof number, Gm is the solutalGrashof number, Pe is the Peclet number owing to temperature and concentration respectively, N is the radiation parameter, S is the heat generation parameter, Sc the Schmidt number, Kr chemical reaction parameter, H(t) is the Heaviside step function.

A close look at the continuity equation shows that the suction velocity normal to the channel is a function of time and shall therefore be taken as;

$$v' = v_0(1 + \epsilon A e^{nt}) \quad (7)$$

The following were obtained;

$$m_4 Re\left(\frac{\partial u}{\partial t} - m_2\frac{\partial u}{\partial y}\right) = \lambda e^{i\omega t} + m_5\frac{\partial^2 u}{\partial y^2} + \left(M^2 + \frac{m_5}{K}\right)u + m_6 GrT + m_6 GmC \quad (8)$$

$\frac{m_1 Pe_t}{\lambda n}\left(\frac{\partial T}{\partial t} - m_2 \frac{\partial T}{\partial y}\right) = \frac{\partial^2 T}{\partial y^2} + \frac{N^2 - S}{\lambda n} T$
(9)
$m_1 Pe_c \left(\frac{\partial C}{\partial t} - m_2 \frac{\partial C}{\partial y}\right) = \frac{\partial^2 C}{\partial y^2} + KrScC$
(10)
where$m_1 = 1 - \phi + \phi \frac{(\rho c_p)_s}{(\rho c_p)_f}, m_2 = \eta(1 + \epsilon A e^{nt}), m_5 = 1 + a\emptyset + b\emptyset^2, m_4 = 1 - \phi + \phi \frac{\rho_s}{\rho_f},$
$m_6 = 1 - \phi + \phi \frac{(\rho\beta)_s}{(\rho\beta)_f}$
with the boundary conditions as;
y=0; u=0, T=0, C=0 (10a)
y=1; u= H(t)$\varepsilon e^{i\omega t}$, T=1, C=1 (10b)
We now assume pertubation solutions for the momentum and temperature of the forms below;
u(y,t)=u_0(y)+u_1(y)$\epsilon e^{i\omega t}$
(11)
T(y,t)=T_0(y)+T_1(y)$\epsilon e^{i\omega t}$ (12)
C(y,t)= C_0(y)+C_1(y)$\epsilon e^{i\omega t}$ (13)
Adopting equations (11) - (13) in equations (8) - (10), we obtain ordinary differential equations depending on the space coordinate only as follows;
$m_5 \frac{d^2 u_0}{dy^2} + m_2 m_4 Re \frac{du_0}{dy} - \left(M^2 + \frac{m_5}{K}\right) u_0 = -m_6 Gr\theta_0$
(14)
$m_5 \frac{d^2 u_1}{dy^2} + m_2 m_4 Re \frac{du_1}{dy} - \left(M^2 + \frac{m_5}{K} + m_4 Rei\omega\right) u_1 = -\lambda - m_6 Gr\theta_1$
(15)
$\frac{d^2 T_0}{dy^2} + \frac{m_2 m_1 Pe}{\lambda n}\frac{dT_0}{dy} + \frac{(N^2 - S)}{\lambda n} T_0 = 0$ (16)
$\frac{d^2 T_1}{dy^2} + \frac{m_2 m_1 Pe}{\lambda n}\frac{dT_1}{dy} + \frac{(-N^2 + S + m_1 Pei\omega)}{\lambda n} T_1 = 0$ (17)
$\frac{d^2 C_0}{dy^2} + m_2 m_1 Pe_c \frac{dC_0}{dy} - KrScC_0 = 0$ (18)
$\frac{d^2 C_1}{dy^2} + m_2 m_1 Pe_c \frac{dC_1}{dy} - (m_1 Pe_c i\omega + KrScC_1) = 0$ (19)
The boundary conditions also as;
y=0; u_0=0,u_1=0, $T_0 = 0, T_1 = 0, C_0 = 0, C_1 = 0$
(20a)
y=1; u_0=0,u_1=H(t), $T_0 = 1, T_1 = 0, C_0 = 1, C_1 = 0$ (20b)
We proceeded to solve equations (14)-(19) together with the appropriate boundary conditions (equation 20a and 20b) and obtained;
u_0(y)=$D_5 e^{\alpha_5 y} + D_6 e^{\alpha_6 y} + D_7 e^{\alpha_1 y} + D_8 e^{\alpha_2 y} + D_9 e^{\alpha_3 y} + D_{10} e^{\alpha_4 y}$ (21)
u_1(y)=$D_{15} e^{\alpha_{11} y} + D_{16} e^{\alpha_{12} y} + D_{17} + D_{18} e^{\alpha_7 y} + D_{19} e^{\alpha_8 y} + D_{20} e^{\alpha_9 y} + D_{21} e^{\alpha_{10} y}$ (22)
T_0(y)=$D_1 e^{\alpha_1 y} + D_2 e^{\alpha_2 y}$ (23)
C_0(y)=$D_3 e^{\alpha_3 y} + D_4 e^{\alpha_4 y}$ (24)
T_1(y)=$D_{11} e^{\alpha_7 y} + D_{12} e^{\alpha_8 y}$ (25)
C_1(y)=$D_{13} e^{\alpha_9 y} + D_{14} e^{\alpha_{10} y}$
(26)

Invoking equations (21)-(26) into equations (11)-(13), we obtain the final solutions for the momentum, energy and specie equations as follows;

u(y,t)=$D_5 e^{\alpha_5 y} + D_6 e^{\alpha_6 y} + D_7 e^{\alpha_1 y} + D_8 e^{\alpha_2 y} + \epsilon\ (D_{15} e^{\alpha_{11} y} + D_{16} e^{\alpha_{12} y} + D_{17} + D_{18} e^{\alpha_7 y} + D_{19} e^{\alpha_8 y}) e^{i\omega t}$
(27)

T(y,t)=$D_1 e^{\alpha_1 y} + D_2 e^{\alpha_2 y} + \epsilon\ (D_{11} e^{\alpha_7 y} + D_{12} e^{\alpha_8 y}) e^{i\omega t}$
(28)

C(y,t)= $D_3 e^{\alpha_3 y} + D_4 e^{\alpha_4 y} + \epsilon\ (D_{13} e^{\alpha_9 y} + D_{14} e^{\alpha_{10} y})\ e^{i\omega t}$
(29)

The constants in the final solutions are clearly stated in the appendix

It is also very crucial to determine the physical effects at the walls of the channel. Hence, we obtain the physical effects by determining the skin friction coefficient and local Nusselt number as follows:

$C_f = \frac{\rho d^2 \tau_w}{\mu^2} = \left(\frac{du}{dy}\right)_{y=0,1}$, $Nu = \frac{d q_w}{k_f (T_w - T_0)} = -\left(\frac{dT}{dy}\right)_{y=0,1}$, $Sh = \frac{d q_w}{k_f (C_w - C_0)} = -\left(\frac{dC}{dy}\right)_{y=0,1}$, where $\tau_w = \mu \left(\frac{du}{dy}\right)_{y=0,d}$, $q_w = -k_f \left(\frac{dT}{dy}\right)_{y=0,d}$

III. RESULTS AND DISCUSSION

Figure 1 shows the effect of Peclet number variation on the temperature and concentration. The increase in the Peclet number shows a significant increase in the temperature and concentration. Figure 2 displays the effect of radiation parameter on the temperature. Increasing the radiation parameter decreases the temperature of the fluid. This is because high radiation of fluid temperature consequently reduces the temperature when it is radiating heat at higher level. Figure 3 depicts the heat generation parameter increase the temperature profile on the increase of heat generation. Figure 4 shows the effective thermal conductivity. Increasing the thermal conductivity increases the fluid temperature. Figure5 depicts the volume fraction of copper nanoparticles. Increase in the volume fraction nanoparticles did not consequently change the temperature of the fluid. Figures 6, 7, 8, 9, 10 show the Peclet number owing to the concentration of the fluid, chemical reaction parameter, Schmidt number, frequency of oscillation and volume fraction of copper respectively, it is seen that incrementally varying the Peclet number, chemical reaction, Schmidt number, frequency of oscillation and volume fraction of copper consequently increase the fluid concentration. Figure 11 presents the increase in the Peclet number increases the velocity of the fluid. The radiation parameter decreases the velocity of the fluid as shown in figure 12 due to a decrease in the momentum boundary layer. Variation in the heat generation and effective thermal conductivity parameters as shown in the figures 13 and 14. Varying the heat generation parameter and effective thermal conductivity did not significantly cause any change in the velocity. Increasing the Reynolds number decreases the velocity of the fluid as shown in figure 15. Figures 16 and 17 show the effect of the chemical reaction parameter and Schmidt number on the velocity profile. It is seen clearly that increasing the chemical reaction parameter and Schmidt number consequently result in no change in the velocity profile. The presence of Lorentz force in the magnetic field deters the motion of the fluid owing to the friction created by the Lorentz force as displays in figure 18. Increasing the Grashof number increases the velocity of the fluid owing the increase in the thermal buoyancy which in turns increases the boundary layer, hence leading to the increase in the velocity of the fluid as seen in figures 19 and 20. The volume fraction of copper nanofluid particles is shown in figure 22. Increasing the volume fraction decreases the fluid velocity. Figure 21 shows an increasing change in the velocity for consequent variation in the porosity on the velocity. Figure 23 shows the impact of the frequency of oscillation on the velocity. Increasing the frequency of oscillation decreases the fluid velocity. The figure 24 shows the different shapes of copper. It is seen that increasing the different shapes of copper decreases the velocity of the fluid.

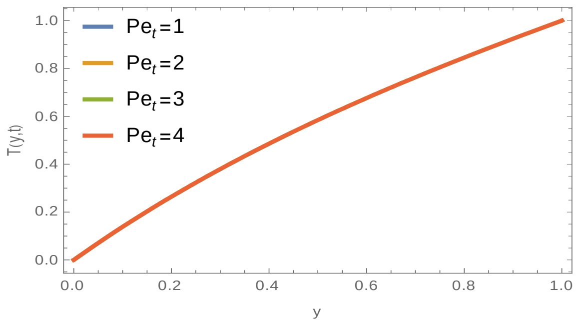

Figure1: Dependence of temperature on coordinate with Peclet number in water based nanofluid when N=1.07, S=0.62, λn=1,t=0.1,$\epsilon = 0.5$

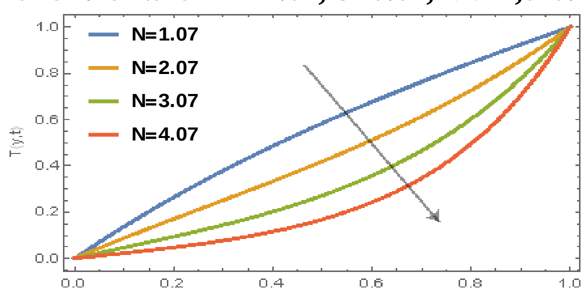

Figure2: Dependence of temperature on coordinate with thermal radiation(N) in water based nanofluid when Pe=1, S=0.62, λn=1,t=0.1,$\epsilon = 0.5$

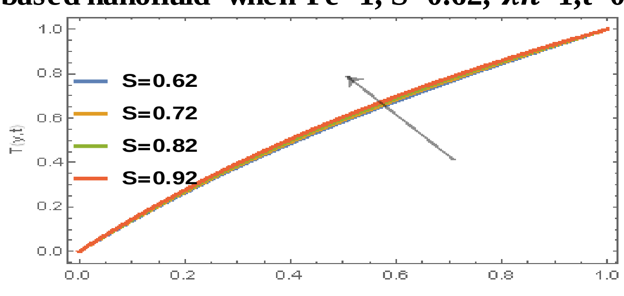

Figure3: Dependence of temperature on coordinate with heat generation parameter in water based nanofluid when N=1.07, Pe=1, λn=1,t=0.1,$\epsilon = 0.5$

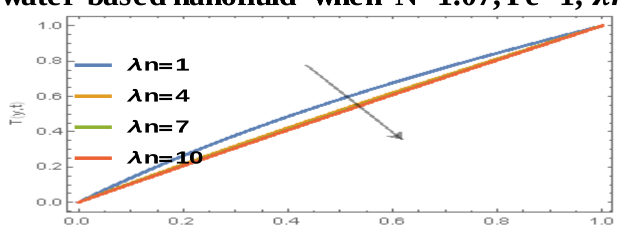

Figure4: Dependence of temperature on coordinate with effective thermal conductivity in water based nanofluid when N=1.07, S=0.62, Pe=1,t=0.1,$\epsilon = 0.5$

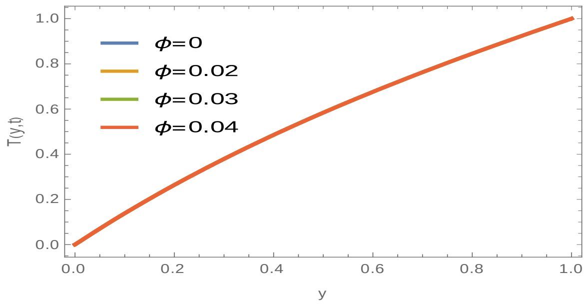

Figure5: Dependence of temperature on coordinate with ϕ of Cu in water based nanofluid when N=1.07, S=0.62, λn=1,t=0.1,$\epsilon = 0.5$

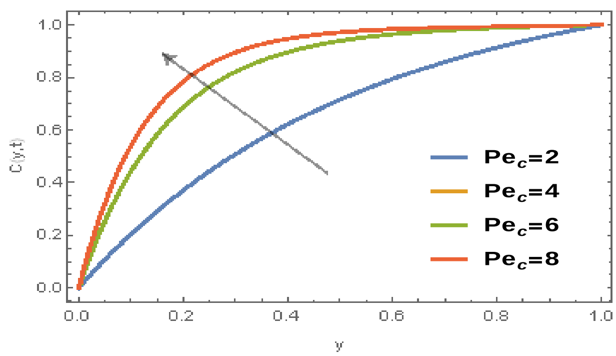

Figure6: Dependence of concentration on coordinate with Pe_c in water based nanofluid when Kr=1.21, Sc=0.15, ω=0.2, t=0.1,$\emptyset = 0$,$\epsilon = 0.5$

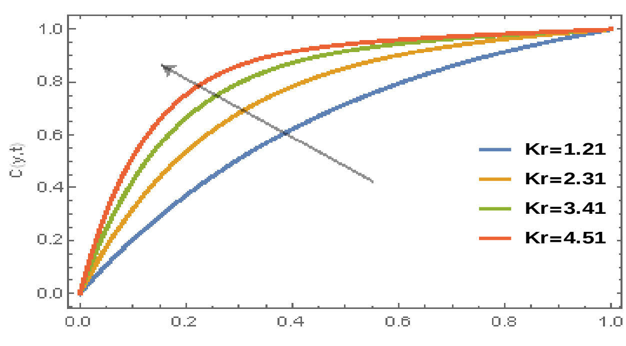

Figure7: Dependence of concentration on coordinate with Kr in water based nanofluid when Pe_c=2, Sc=0.15, ω=0.2, t=0.1,$\emptyset = 0$,$\epsilon = 0.5$

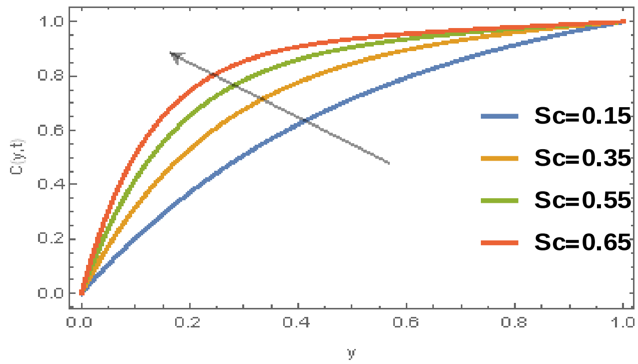

Figure8: Dependence of concentration on coordinate with Sc in water based nanofluid when Pe_c=2, Kr=1.21, ω=0.2, t=0.1,$\emptyset = 0, \epsilon = 0.5$

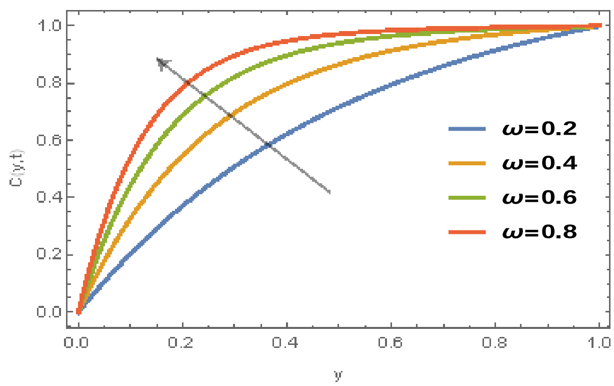

Figure9: Dependence of concentration on coordinate with ω in water based nanofluid when Pe_c=2, Sc=0.15, Kr=1.21, ω=0.2, t=0.1,$\emptyset = 0, \epsilon = 0.5$

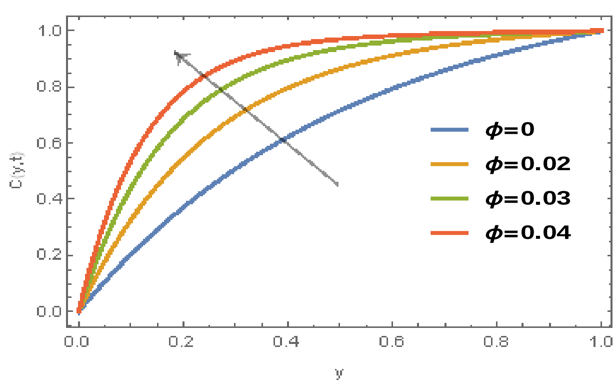

Figure10: Dependence of concentration on coordinate with $\emptyset$ of Cu in water based nanofluid when Pe_c=2, Sc=0.15, Kr=1.21, ω=0.2, t=0.1,$\emptyset = 0, \epsilon = 0.5$

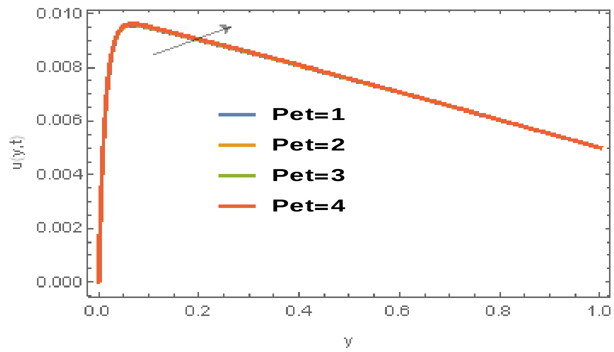

Figure11: Dependence of velocity on coordinate with Peclet number in water based nanofluid when N=1.07, S=0.62, λn=1,t=0.1,$\epsilon = 0.5$,Gr=0.03,M=10,K=1.49,Re=100, $\omega = 0.2$,,$Pe_c = 2$, Gm=0.05,Sc=0.15, $\emptyset = 0$, Kr=1.21

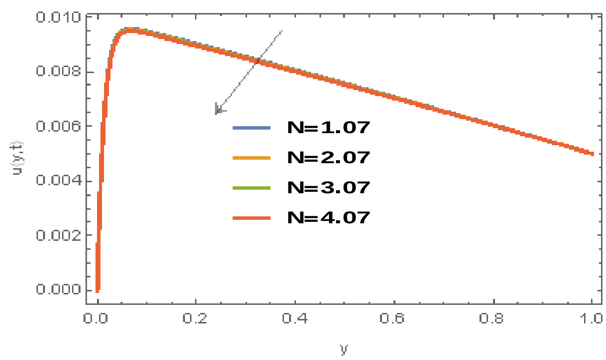

Figure12: Dependence of velocity on coordinate with N in water based nanofluid when S=0.62, λn=1,t=0.1,$\epsilon = 0.5$,Gr=0.03,M=10,K=1.49,Re=100, $\omega = 0.2$,$Pe_t = 1$,$Pe_c = 2$, Gm=0.05,Sc=0.15, $\emptyset = 0$, Kr=1.21

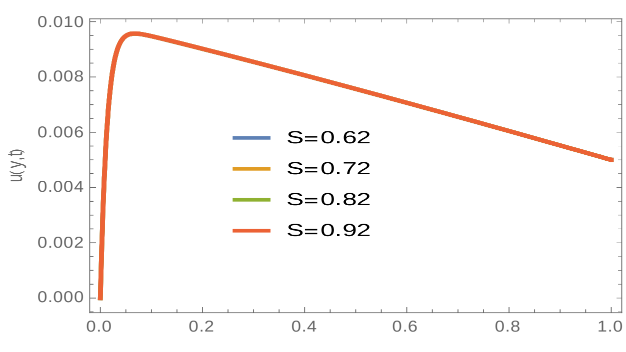

Figure13: Dependence of velocity on coordinate with S in water based nanofluid when N=1.07,, λn=1,t=0.1,$\epsilon = 0.5$,Gr=0.03,M=10,K=1.49,Re=100, $\omega = 0.2$,$Pe_t = 1$,$Pe_c = 2$, Gm=0.05,Sc=0.15, $\emptyset = 0$, Kr=1.21

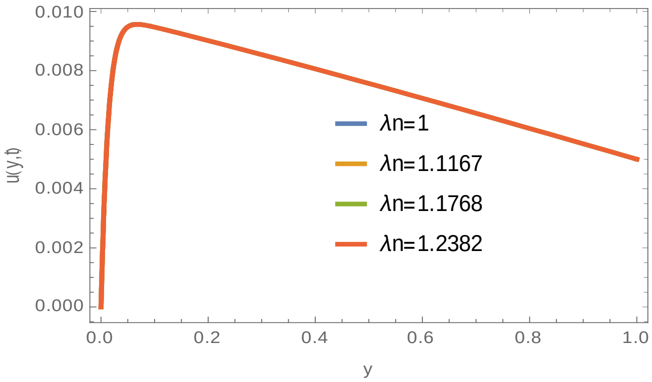

Figure14: Dependence of velocity on coordinate with effective thermal conductivity in water based nanofluid when N=1.07, S=0.62,t=0.1,$\epsilon = 0.5$,Gr=0.03,M=10,K=1.49,Re=100, $\omega = 0.2$,$Pe_t = 1$,$Pe_c = 2$, Gm=0.05,Sc=0.15, $\emptyset = 0$, Kr=1.21

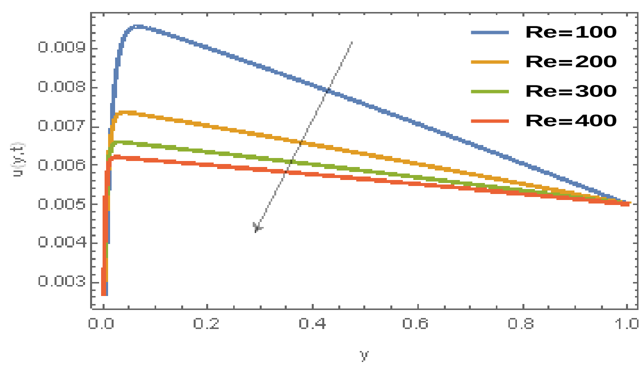

Figure15: Dependence of velocity on coordinate with Reynolds number in water based nanofluid when N=1.07, S=0.62, λn=1,t=0.1,$\epsilon = 0.5$,Gr=0.03,M=10,K=1.49, $\omega = 0.2$,$Pe_t = 1$,$Pe_c = 2$, Gm=0.05,Sc=0.15, $\emptyset = 0$, Kr=1.21

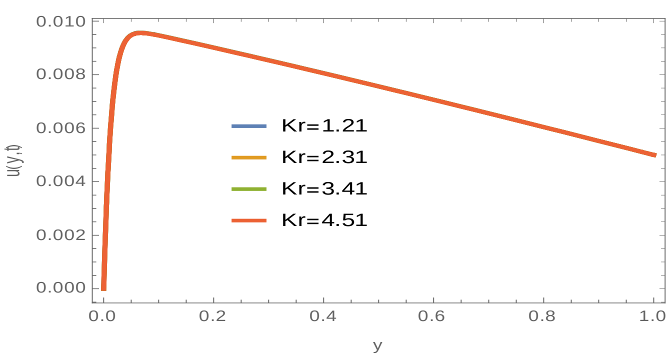

Figure16: Dependence of velocity on coordinate with Chemical reaction parameter in water based nanofluid when N=1.07, S=0.62, λn=1,t=0.1,$\epsilon = 0.5$,Gr=0.03,M=10,K=1.49,Re=100, $\omega = 0.2$,$Pe_t = 1$,$Pe_c = 2$, Gm=0.05,Sc=0.15, $\emptyset = 0$

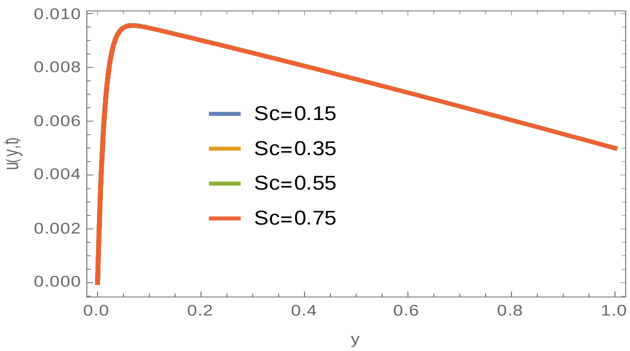

Figure17: Dependence of velocity on coordinate with Schmidt number in water based nanofluid when N=1.07, S=0.62, λn=1,t=0.1,$\epsilon = 0.5$,Gr=0.03,M=10,K=1.49,Re=100, $\omega = 0.2$,$Pe_t = 1$,$Pe_c = 2$, Gm=0.05, $\emptyset = 0$, Kr=1.21

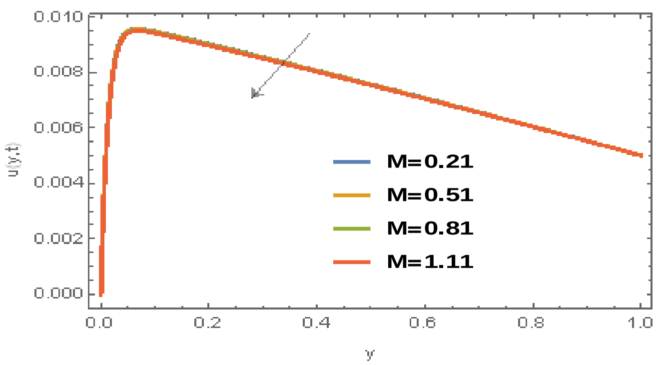

Figure18: Dependence of velocity on coordinate with M in water based nanofluid when N=1.07, S=0.62, λn=1,t=0.1,$\epsilon = 0.5$,Gr=0.03,M=10,K=1.49,Re=100, $\omega = 0.2$,$Pe_t = 1$,$Pe_c = 2$, Gm=0.05,Sc=0.15, $\emptyset = 0$, Kr=1.21

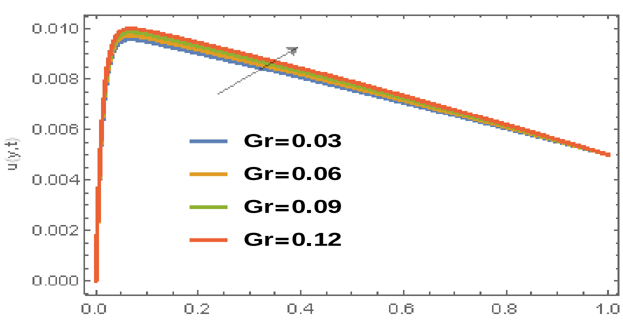

Figure19: Dependence of velocity on coordinate with Gr in water based nanofluid when N=1.07, S=0.62, λn=1,t=0.1,$\epsilon = 0.5$, M=10,K=1.49,Re=100, $\omega = 0.2$,$Pe_t = 1$,$Pe_c = 2$, Gm=0.05,Sc=0.15, $\emptyset = 0$, Kr=1.21

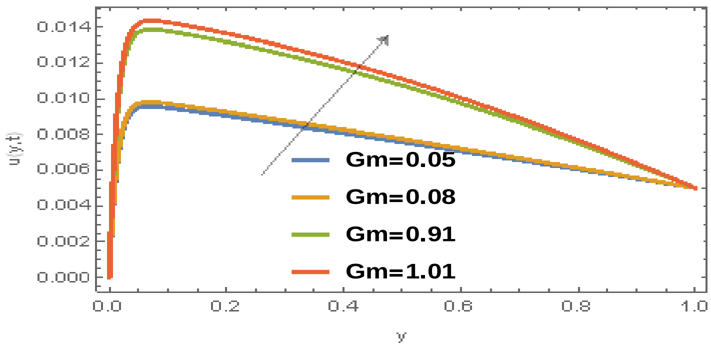

Figure20: Dependence of velocity on coordinate with Gm in water based nanofluid when N=1.07, S=0.62, λn=1,t=0.1,$\epsilon = 0.5$,Gr=0.03,M=10,K=1.49,Re=100, $\omega = 0.2$,$Pe_t = 1$,$Pe_c = 2$,Sc=0.15, $\emptyset = 0$, Kr=1.21

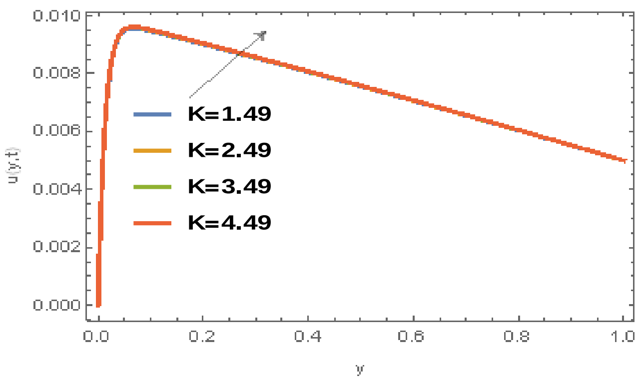

Figure21: Dependence of velocity on coordinate with K in water based nanofluid when N=1.07, S=0.62, λn=1,t=0.1,$\epsilon = 0.5$,Gr=0.03,M=10 ,Re=100, $\omega = 0.2$,$Pe_t = 1$,$Pe_c = 2$, Gm=0.05,Sc=0.15, $\emptyset = 0$, Kr=1.21

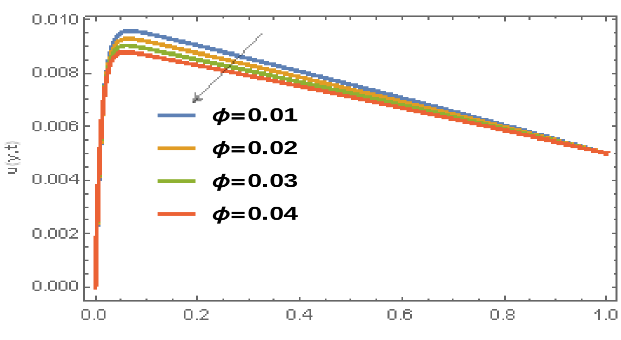

Figure22: Dependence of velocity on coordinate with $\emptyset$ of Cu in water based nanofluid when N=1.07, S=0.62, λn=1,t=0.1,$\epsilon = 0.5$,Gr=0.03,M=10,K=1.49,Re=100, $\omega = 0.2$,$Pe_t = 1$,$Pe_c = 2$, Gm=0.05,Sc=0.15 , Kr=1.21

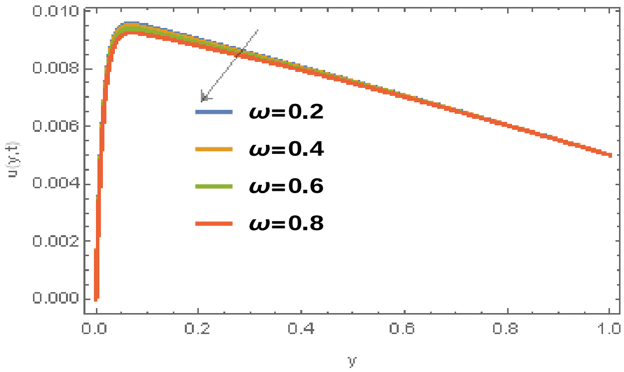

Figure23: Dependence of velocity on coordinate with ω in water based nanofluid when N=1.07, S=0.62, λn=1,t=0.1,$\epsilon = 0.5$,Gr=0.03,M=10,K=1.49,Re=100,$Pe_t = 1$,$Pe_c = 2$, Gm=0.05,Sc=0.15 , Kr=1.21, $\emptyset = 0$

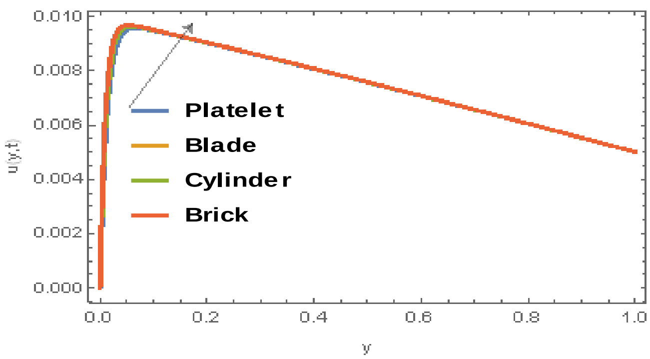

Figure24: Dependence of velocity on coordinate with shape factors in water based nanofluid when N=1.07, S=0.62, λn=1,t=0.1,$\epsilon = 0.5$,Gr=0.03,M=10,K=1.49,Re=100,$Pe_t = 1$,$Pe_c = 2$, Gm=0.05,Sc=0.15 , Kr=1.21, $\emptyset = 0$

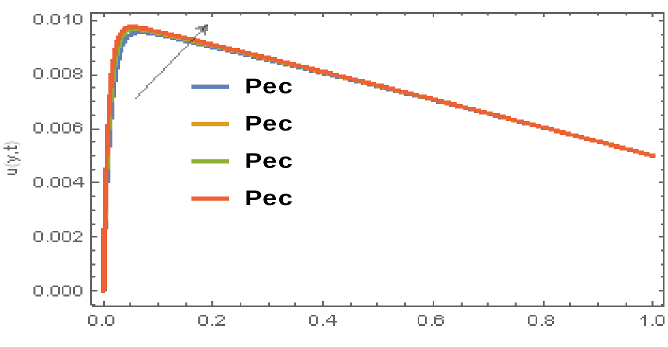

Figure25: Dependence of velocity on coordinate withPe_c in water based nanofluid when N=1.07, S=0.62, λn=1,t=0.1,$\epsilon = 0.5$,Gr=0.03,M=10,K=1.49,Re=100,$Pe_t = 1$, Gm=0.05,Sc=0.15 , Kr=1.21, $\emptyset = 0$

IV. CONCLUSION

In this paper, we have successfully analyzed the energy transfer in dual mhd convection of heat and mass flow of cu – h_2o nanofluid in a porous channel with oscillating upper plate

. The governing equations were analytically solved and expressed in exponential and complimentary functions. From the foregoing, it is observed that:

1. Thermal radiation decreased the temperature of the fluid.
2. Heat generation/absorption parameter increased the temperature of the fluid.
3. The effective thermal conductivity increased the temperature of the fluid.
4. Peclet number decreased the velocity of the fluid.
5. Reynolds number decreased the fluid velocity.
6. Peclet number, Reynolds number and heat generation rapidly increased and decreased the entropy generation at the lower and upper plates respectively.
7. Increasing the volume fraction of copper leads to an increase in the concentration of the fluid.

REFERENCES

Aaiza, G.; Khan, I &Shafie, S.(2015). Energy transfer in mixed convection MHD flow of nanofluid containing different shapes of nanoparticles in a channel filled with saturated porous medium. Nanoscale research letters,2(2015), 1-16.

Achogo, W. H.; Adikabu, I. N.; Awortu, I. &Eleonu, B. C.(2020). Soret effect on MHD free convection through a porous inclined channel in the presence of thermal radiation. International journal of research and innovation in applied, 5(7),117-124.

Buggaramulu J. &Venkata M. K.(2017). MHD convection flow of Kuvshinski fluid past an infinite vertical porous plate with radiation and chemical reaction effects. International journal on recent and innovation trends in computing and communication, 5(9),64-74.

Choi SUS (1995). Enhancing thermal conductivity of fluids with nanoparticle, in: D.A. Siginer, H.P. Wang (Eds.), Developments and Applications of Non- Newtonian Flows. ASME FED, 66(1995),99–105.

Kathyayani, G. & Praveen B.D.M.(2016). Heat and mass transfer on mhd flow over an infinite rotating oscillating vertical porous plate. International journal of advanced research, 4(6),1078-1086. DOI:10.21474/IJAR01

Khan, S. M.; Karim, I; Ali, E. L. & Islam, A.(2012). Unsteady MHD free convection boundary – layer flow of a nanofluid along a stretching sheet with thermal radiation and viscous dissipation effects. International nano letters, 2(2012), 1-9.

Latiff, N. A.; Uddin, M. J. & Ismail, A. I.(2016). Stefan blowing effect on bioconvective flow of nanofluid over a solid rotating stretchable disk. Propulsion and power research, 5(4), 267-278.

Madhura, K. R.; Babitha. A. &Iyenga, S. S.(2017). Impact of heat and mass transfer on mixed convective flow of nanofluid through porous medium. International Journal of Applied Computational Mathematics, 10(2), 10-11. DOI:10.1007/s40819-017-0424-3

Madhura, K. R.; Kalpana, G. &Soniya, H.(2020). Heat and mass transfer of MHD fluid flow under the influence of radiative effect and different pressure gradients. Studies in Indian Place Names,40(10),427-439.

Malvandi, A.; Ganji, D. D.; Hedayati, F & Rad, Y. E.(2013). An analytical study on entropy generation of nanofluids over a flat plate.Alexandria engineering journal, 52(2013), 595-604.

Murugesan, T. & Kumar, D. M.(2019). Viscous dissipation and joule heating effects on MHD flow of a thermo-solutal stratified nanofluid over an exponentially stretching sheet with radiation and heat generation/absorption. World schientific news, 129(2019),193-210.

Naik, M. T. &Sundar, L. S. (2011). Investigation into thermophysical properties of glycol based CuOnanofluid for heat transfer applications. World AcadScience Engineer Technology, 59(2011),,440–446.

Reddy M. G. & Reddy N. B.(2011). Mass transfer and heat generation effects on MHD free convection flow past an inclined vertical surface in a porous medium. Journal of applied fluid mechanics, 4(2), 7-11.

Sharma R. &Isahk, A.(2014). Second order slip flow of Cu-Water nanofluid over a stretching sheet with heat transfer. WSEAS transactions on fluid mechanics, 9(2014), 26-33.

Shateyi, S.; Motsa, S. S. &Makukula, Z.(2015). On spectral relaxation method for entropy generation on MHD flow and heat transfer of a Maxwell fluid. Journal of applied fluid mechanics, 8(1), 21-31.

Srinivasacharya, D. &Bindu H. K.(2015). Entropy generation in a micropolar fluid flow through an inclined channel.Alexandria engineering journal, 55(2016), 973-982.

Vajjha, R.S. & Das, D.K .(2009). Experimental determination of thermal conductivity of three nanofluids and development of new correlations. International journal of heat and mass transfer,, 52(2009), 4675-4682.

APPENDIX

$$\alpha_1 = \frac{\frac{-m_2 m_1 Pe}{\lambda n} + \sqrt{\left(\frac{m_2 m_1 Pe}{\lambda n}\right)^2 - 4\left(\frac{N^2 - S}{\lambda n}\right)}}{2}, \qquad \alpha_7 = \frac{\frac{-m_2 m_1 Pe}{\lambda n} + \sqrt{\left(\frac{m_2 m_1 Pe}{\lambda n}\right)^2 - 4\left(\frac{m_1 Pei\omega - N^2 + S}{\lambda n}\right)}}{2},$$

$$\alpha_2 = \frac{\frac{-m_2 m_1 Pe}{\lambda n} - \sqrt{\left(\frac{m_2 m_1 Pe}{\lambda n}\right)^2 - 4\left(\frac{N^2 - S}{\lambda n}\right)}}{2}, \qquad D_{11} = D_{12} = 0, \qquad \alpha_{11} = \frac{-m_2 m_4 Re + \sqrt{(m_2 m_4 Re)^2 - 4\left(M^2 + \frac{m_5}{K} + m_4 Rei\omega\right)}}{2m_5},$$

$$\alpha_8 = \frac{\frac{-m_2 m_1 Pe}{\lambda n} - \sqrt{\left(\frac{m_2 m_1 Pe}{\lambda n}\right)^2 - 4\left(\frac{m_1 Pei\omega - N^2 + S}{\lambda n}\right)}}{2}, \alpha_{12} = \frac{-m_2 m_4 Re - \sqrt{(m_2 m_4 Re)^2 - 4\left(M^2 + \frac{m_5}{K} + m_4 Rei\omega\right)}}{2m_5}$$

$$D_2 = \frac{1}{e^{\alpha_2} - e^{\alpha_1}}, \qquad D_{18} = \frac{-m_6 Gr D_{11}}{m_5 \alpha_7{}^2 + -m_2 m_4 Re \alpha_7 - \left(M^2 + \frac{m_5}{K} + m_4 Rei\omega\right)}, \qquad D_{19} = \frac{-m_6 Gr D_{11}}{m_5 \alpha_8{}^2 + -m_2 m_4 Re \alpha_8 - \left(M^2 + \frac{m_5}{K} + m_4 Rei\omega\right)} D_{17} = \frac{\lambda}{\left(M^2 + \frac{m_5}{K} + m_4 Rei\omega\right)},$$

$$D_1 = \frac{-1}{e^{\alpha_2} - e^{\alpha_1}}, \alpha_5 = \frac{-m_2 m_4 Re + \sqrt{(m_2 m_4 Re)^2 - 4m_5\left(M^2 + \frac{m_5}{K}\right)}}{2m_5}, \alpha_6 = \frac{-m_2 m_4 Re - \sqrt{(m_2 m_1 Re)^2 - 4m_5\left(M^2 + \frac{m_5}{K}\right)}}{2m_5},$$

$$D_7 = \frac{m_6 Gr A_1}{m_5 \alpha_1{}^2 + -m_2 m_4 Re \alpha_1 - \left(M^2 + \frac{m_5}{K}\right)}, D_8 = \frac{-m_6 Gr A_1}{m_5 \alpha_2{}^2 + -m_2 m_4 Re \alpha_2 - \left(M^2 + \frac{m_5}{K}\right)},$$

$$D_6 = \frac{1}{e^{\alpha_6} - e^{\alpha_5}}\left[D_7 e^{\alpha_5 y} + D_8 e^{\alpha_5 y} - D_7 e^{\alpha_1 y} - D_8 e^{\alpha_2 y}\right], \qquad D_5 = \frac{1}{e^{\alpha_6} - e^{\alpha_5}}\left[D_7 e^{\alpha_5 y} + D_8 e^{\alpha_5 y} - D_7 e^{\alpha_1 y} - D_8 e^{\alpha_2 y}\right] - [D_7 + D_8],$$